Supporting Information

Spherical Nucleic Acid Vaccine Structure Markedly Influences Adaptive Immune Responses of Clinically-Utilized Prostate Cancer Targets

Michelle H. Teplensky, Jasper W. Dittmar, Lei Qin, Shuya Wang, Michael Evangelopoulos, Bin Zhang, Chad A. Mirkin**

Supplementary Table S1. Sequences of DNA used in this paper.
(PO = phosphate backbone; PS = phosphorthioate backbone; Sp18 = 18-O-Dimethoxytritylhexaethyleneglycol,1-[(2-cyanoethyl)-(N,N-diisopropyl)]-phosphoramidite (Glen research #10-1918); Cholesterol = 3'-Cholesteryl-TEG CPG (Glen research # 20-2975); Thiol = 3'-Thiol-Modifier C3 S-S CPG (Glen research # 20-2933); Cy5 = 1-[3-(4-monomethoxytrityloxy)propyl]-1'-[3-[(2-cyanoethyl)-(N,N-diisopropylphosphoramidityl]propyl]-3,3,3',3'-tetramethylindodicarbocyanine chloride (Glen research #10-5915)

Name	Sequence (5'→3')	Backbone	Molecular weight	Ext. Coeffecient[1] L/(mole·cm)
CpG 1826-3'Chol adjuvant (mouse)	TCC ATG ACG TTC CTG ACG TT $(Sp18)_2$ Cholesterol	PS	7809	181100
CpG 1826-3'SH Complement (mouse)	AAC GTC AGG AAC GTC ATG GA Thiol	PO	6329	206700
CpG 1826-3'SH Complement with spacer (mouse)	AAC GTC AGG AAC GTC ATG GA Sp18 Thiol	PO	6674	206700
CpG 1826-3'Chol adjuvant fluorescent (mouse)	TCC ATG ACG TTC CTG ACG TT Cy5 $(Sp18)_2$ Cholesterol	PS	8343	191100
CpG 7909-3'Chol adjuvant (human)	TCG TCG TTT TGT CGT TTT GTC GTT $(Sp18)_2$ Cholesterol	PS	9142	209400
CpG 7909-3'SH Complement with spacer (human)	AAC GAC AAA ACG ACA AAA CGA CGA Sp18 Thiol	PO	7873	259000
CpG 7909-3'Chol adjuvant fluorescent (human)	TCG TCG TTT TGT CGT TTT GTC GTT Cy5 $(Sp18)_2$ Cholesterol	PS	9676	219400

[1]Calculated using IDT's Oligoanalyzer Tool: https://www.idtdna.com/calc/analyzer

Supplementary Table S2. Sequences of Peptides used in this paper.

Name	Sequence (N terminus -> C terminus)	Molecular weight
$PSMA_{711-719}$	CALFDIESKV	1124
$TARP_{29-37-9V}$	CFLRNFSLMV	1230

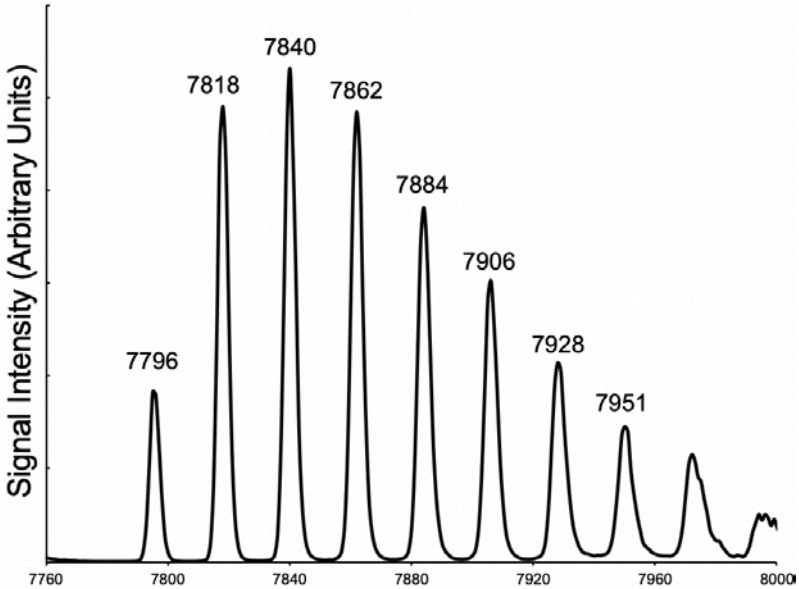

Supplementary Figure S1. ESI-MS spectrum of the purified $PSMA_{711\text{-}719}$ peptide-DNA conjugate used to generate the SNA structure. Expected product mass is 7796.

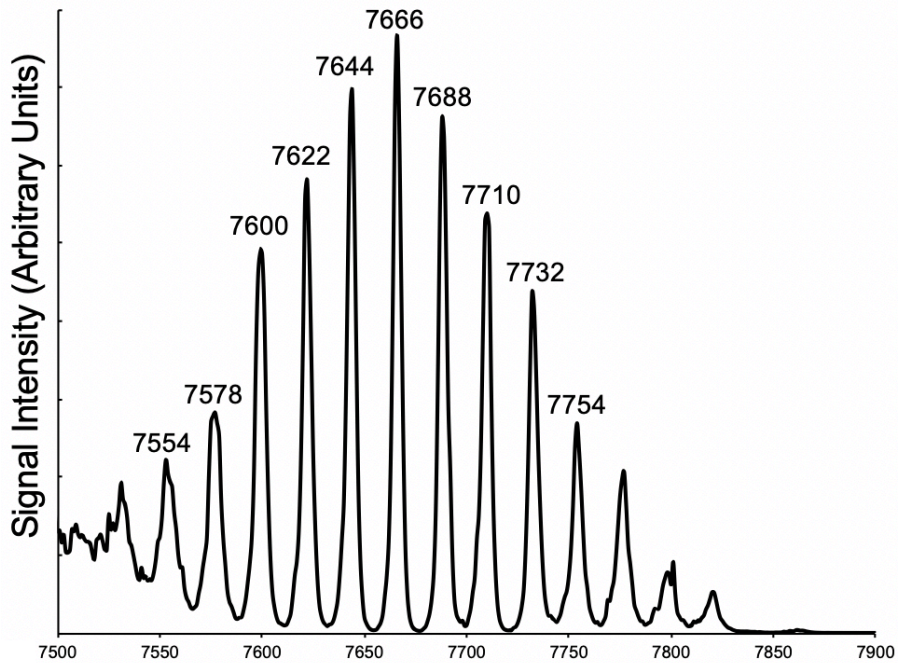

Supplementary Figure S2. ESI-MS spectrum of the purified $TARP_{29\text{-}37\text{-}9V}$ peptide-DNA conjugate used to generate the SNA structure. Expected product mass is 7557.

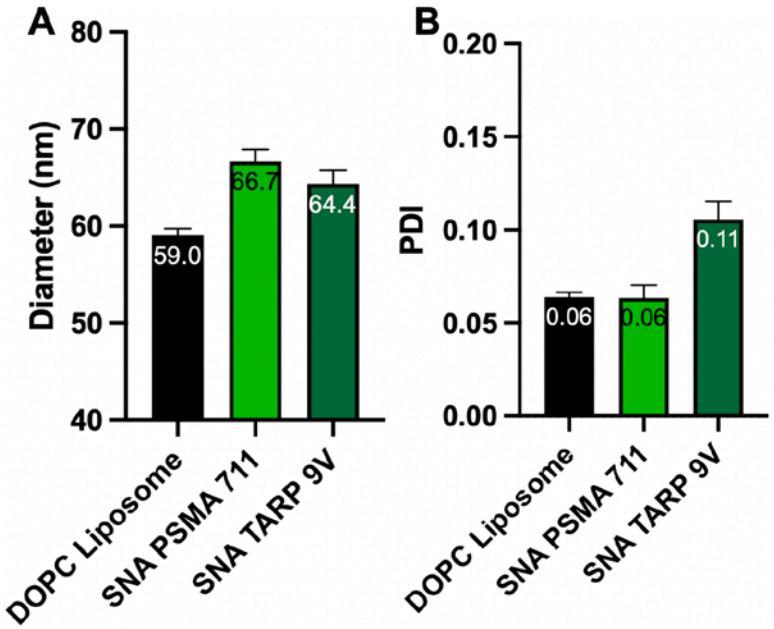

Supplementary Figure S3. Dynamic light scattering (DLS) characterization of bare liposomes and SNAs using a Malvern Zetasizer. A) Hydrodynamic diameter of bare liposomes and SNAs. B) Polydispersity index (PDI) of bare liposomes and SNAs. Mean ± SEM shown for n = 5.

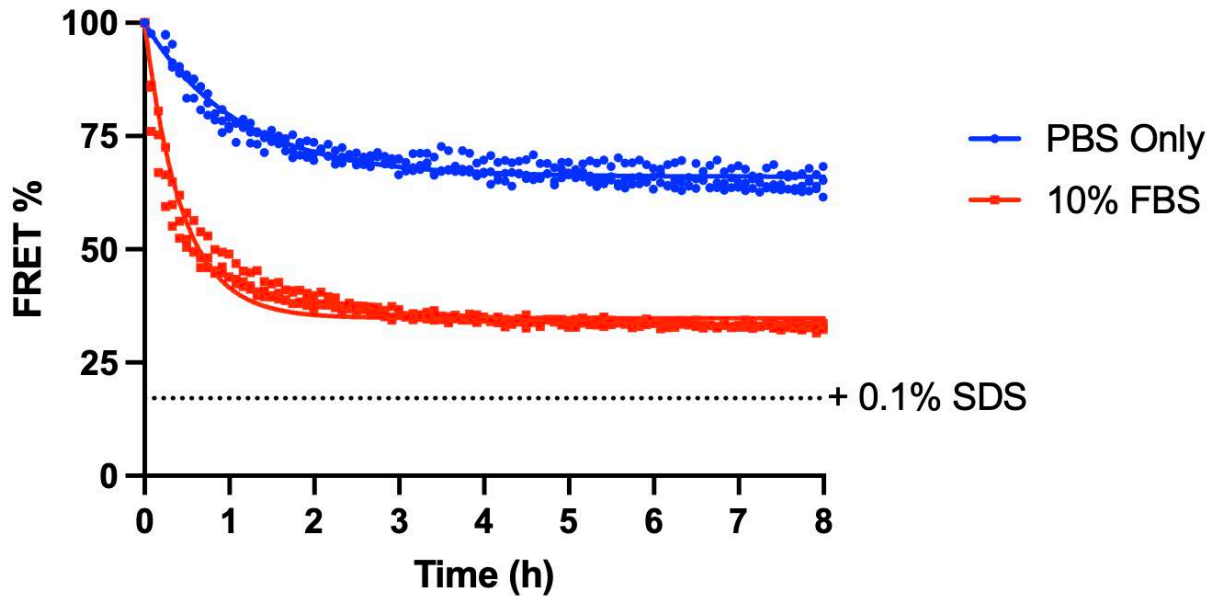

Supplementary Figure S4. Evaluation of SNA stability in PBS and serum. SNAs were synthesized to track the association of the shell of duplexed DNA and peptide to the liposome core in a complex biological milieu. A monoexponential decay of FRET % was observed after incubation with 10% FBS (half-life ~18 min). The reduction in signal after incubation with PBS sample can be attributed to sample evaporation over extended time, also contributing to some of the FRET % reduction when sample is incubated with 10% FBS. The additional reduction in signal in serum is likely due to dissociation of the shell from the core as a result of serum proteins. The addition of 0.1 % SDS disrupts all liposomes and leads to full dissociation. It can be observed that this baseline level is lower than the signal of SNAs in 10 % FBS after 8 h, indicating that there is still a shell of duplex on the surface of the SNA even at 8 hours.

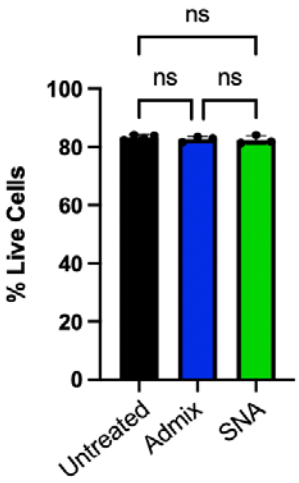

Supplementary Figure S5. *In vitro* cytotoxicity for different vaccines. SNA and admix vaccines exhibited no toxicity compared to untreated cells after incubation with hPBMCs. Data is presented as mean ± SD with n = 3 - 4 per group. Significance was analyzed using one-way ANOVA followed by Tukey's multiple comparisons test. Ns=non-significant.

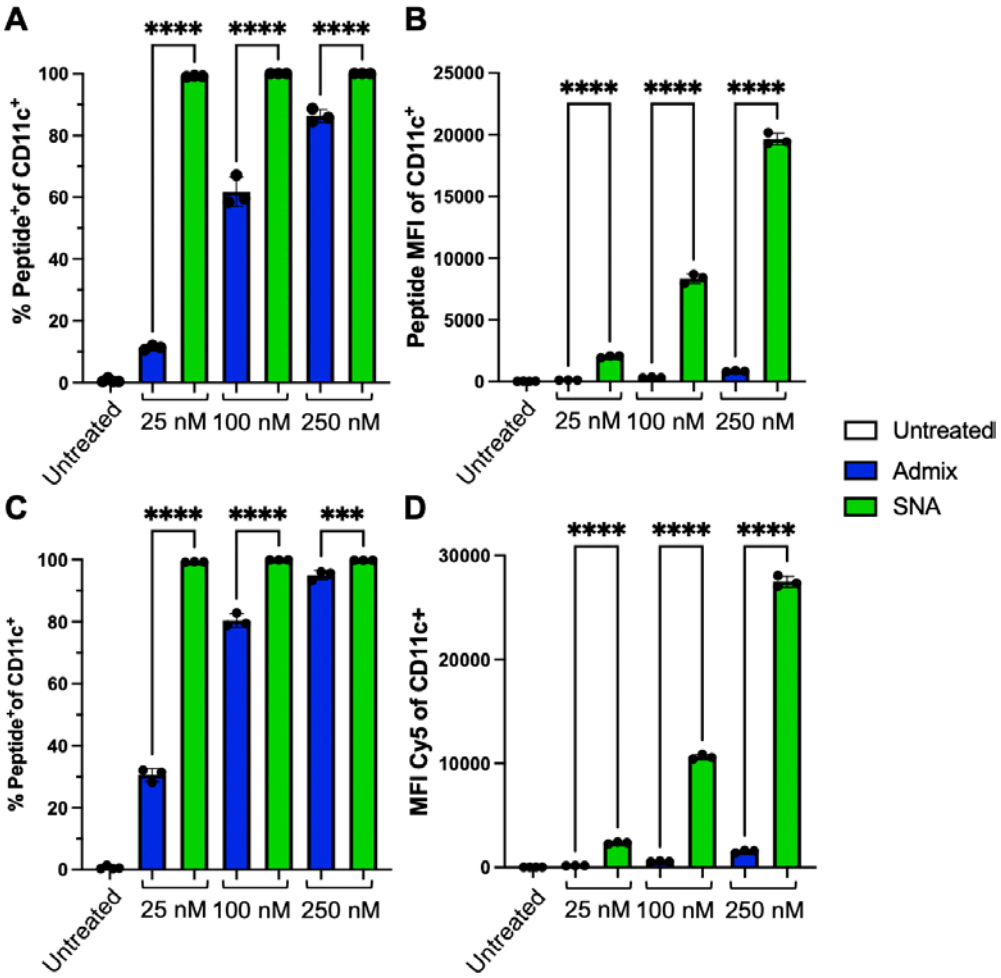

Supplementary Figure S6. *In vitro* uptake of vaccines into hPBMCs. Vaccines containing fluorescent labels were incubated for (A, B) 1 h or (C, D) 4 h with hPBMCs and assessed for the (A, C) percentage of $CD11c^+$ DCs containing peptide and (B, D) the amount of peptide taken up into $CD11c^+$ DCs. All data is presented as mean ± SD with n = 3 - 4 per group. Significance between groups was analyzed using one-way ANOVA followed by Tukey's multiple comparisons test. ****p<0.0001.

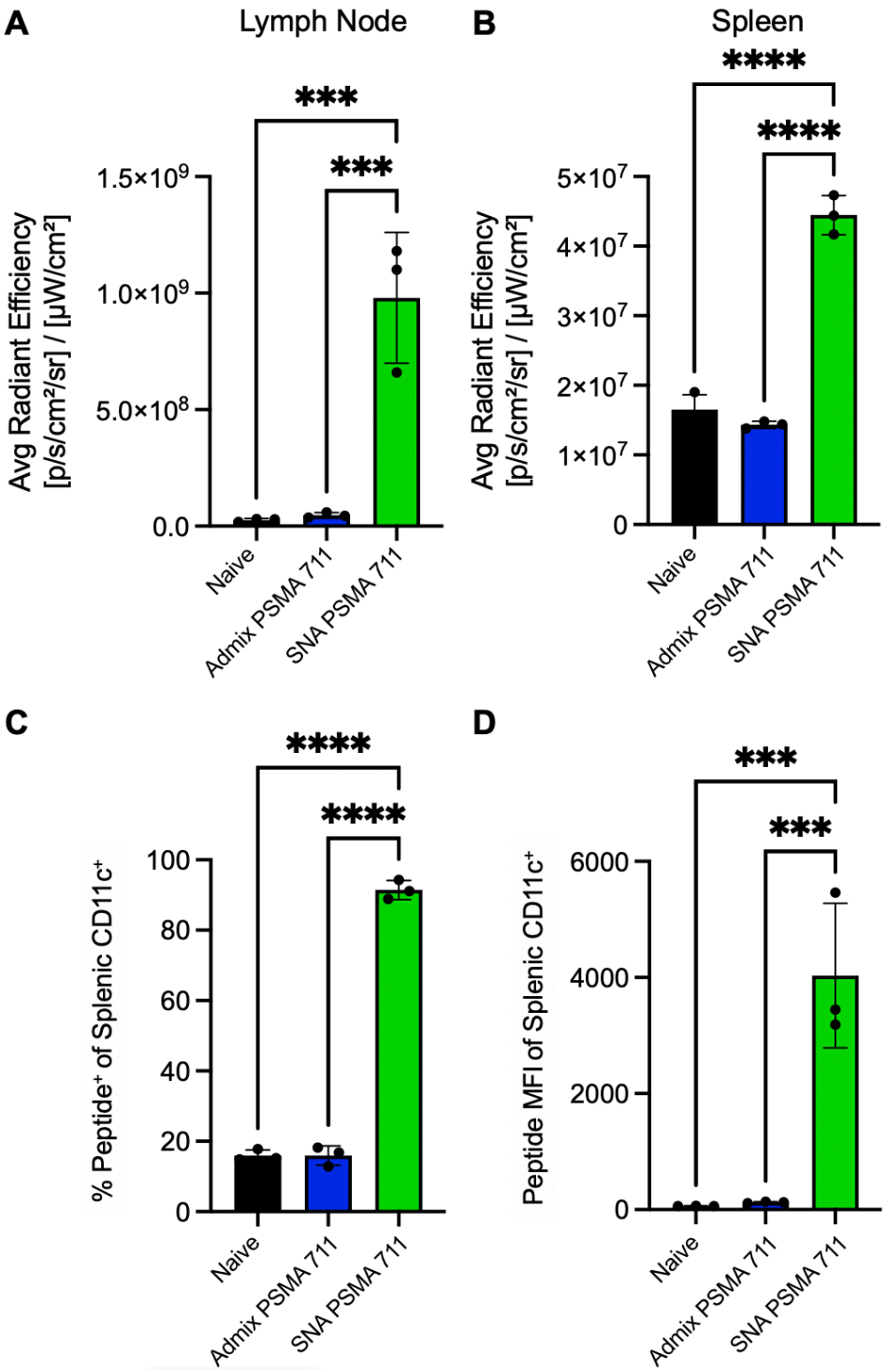

Supplementary Figure S7. *In vivo* distribution of vaccines. Vaccines containing fluorescent labels for tracking were injected subcutaneously into mice and uptake after 24 h into organs containing high populations of immune cells was assessed *via* IVIS. Peptide antigen uptake into the (A) lymph nodes and (B) spleen was significantly enhanced through delivery on the SNA platform compared to the free peptide in a simple mixture solution. Spleens were harvested and isolated into single cell suspensions and the $CD11c^+$ dendritic cell population was assessed for peptide uptake. Both the (C) percentage of $CD11c^+$ DCs containing peptide and the (D) amount of peptide in the cells was significantly elevated through the SNA. All data is presented as mean ± SD with n = 3 per group. Significance between groups is shown and was analyzed using one-way ANOVA followed by Tukey's multiple comparisons test to analyze differences between treatment groups. ***$p<0.001$; ****$p<0.0001$.

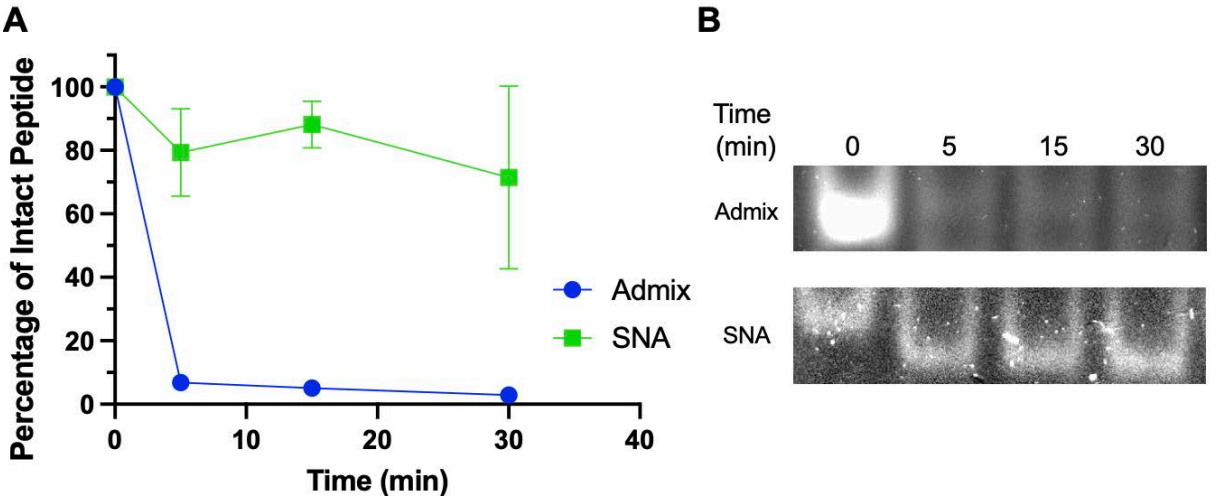

Supplementary Figure S8. Peptide resistance to degradation. (A) Densitometry analysis of intensity of Cy5 signal from Native PAGE gels indicating the amount of peptide antigen present over time after incubation with Proteinase K, a serine protease capable of cleaving multiple peptide bonds, with specifically six predicted cleavage sites for the employed $PSMA_{711}$ peptide.[2] The SNA structure enhances the percentage of uncleaved intact peptide over the course of the study compared to the free peptide as formulated in an admix, which is nearly fully degraded at the first measured timepoint (5 min). Data is presented as mean ± SD with n = 3 per group per timepoint. (B) One representative Native PAGE gel of timepoints.
[2]Calculated using Swiss Institute of Bioinformatics (SIB)'s ExPASy: PeptideCutter: https://web.expasy.org/cgi-bin/peptide_cutter/peptidecutter.pl

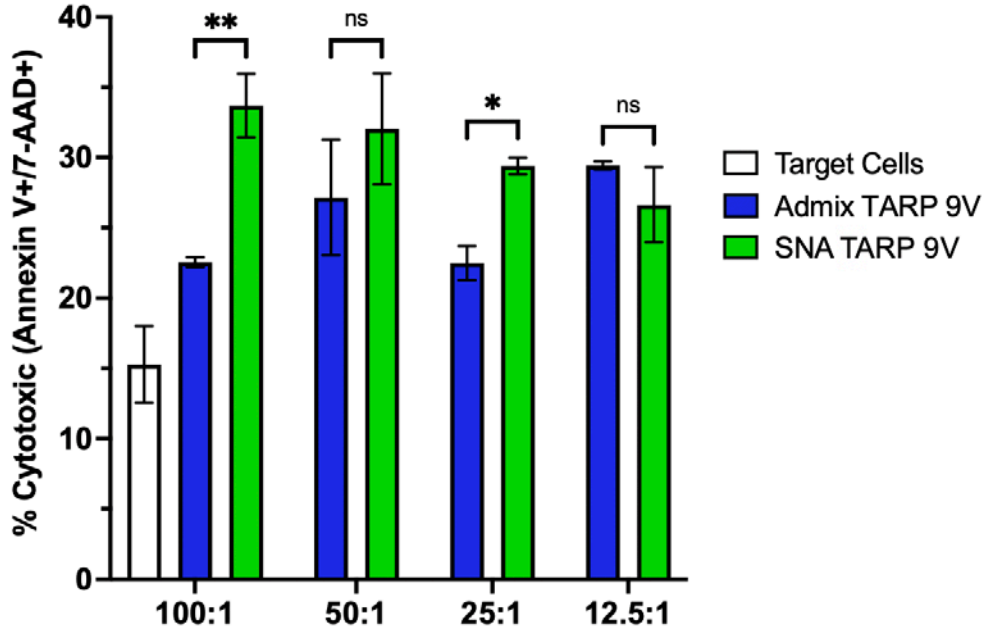

Supplementary Figure S9. Splenic $CD8^+$ T cell killing ability targeting MCF-7 cells e*x vivo*. T cells raised from mice immunized with $TARP_{29\text{-}37\text{-}9V}$ formulations were co-cultured at different effector to target (T cell/target cells, E/T) ratios with MCF-7 cells, which natively express TARP. Apoptosis and necrosis quantified *via* Annexin V and 7-aminoactinomycin D (7-AAD) after 24 h co-culture. All data is presented as mean ± SD with n = 3 per treatment group. Significance between groups is shown and was analyzed using two-way ANOVA followed by Sidak's multiple comparisons test to analyze differences between treatment groups at each ratio. *p<0.05; **p<0.01; ns=non-significant.

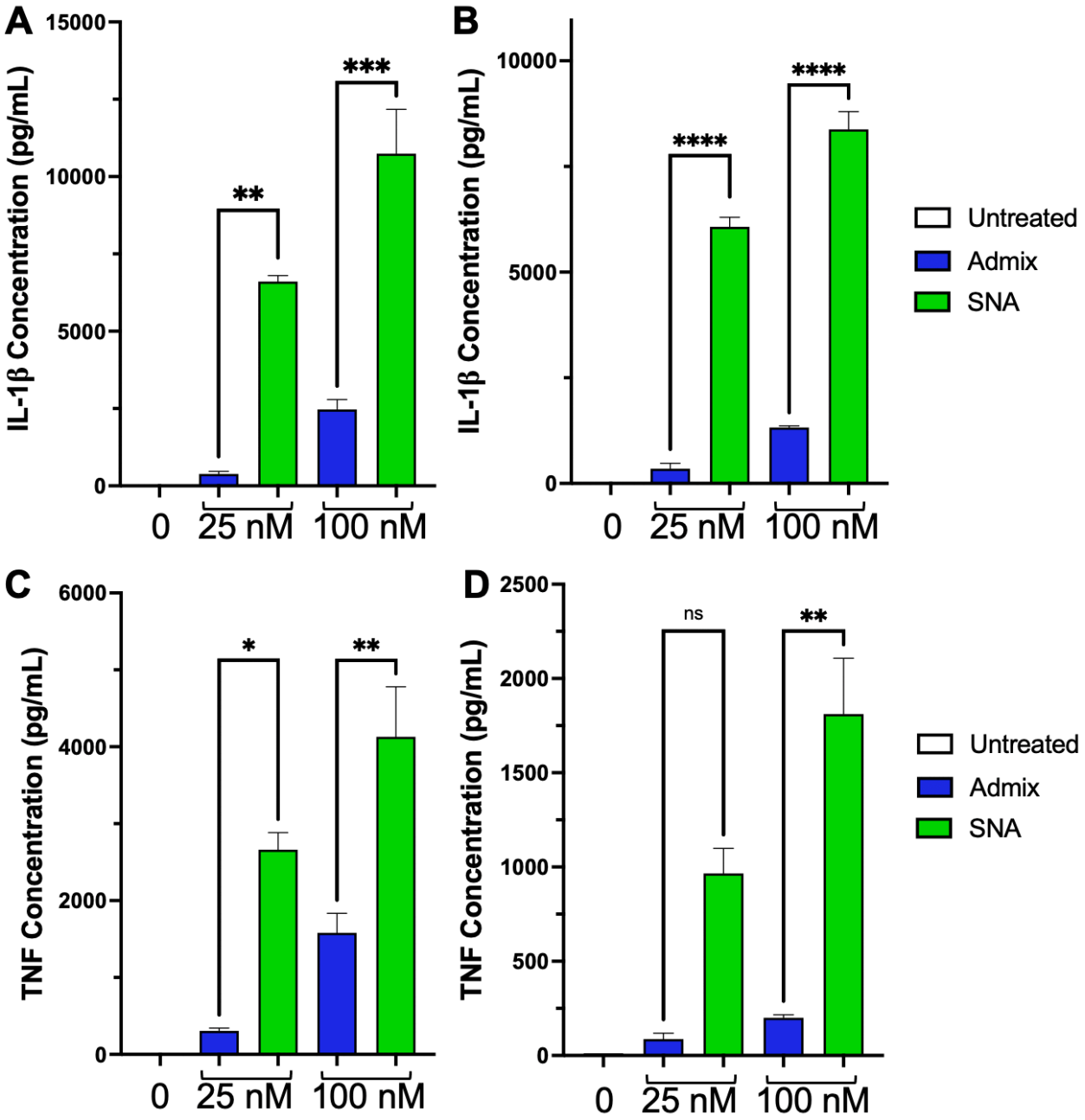

Supplementary Figure S10. Cytokine production through activation of human PMBCs. Secretion of cytokines was assessed from the supernatant after (A, C) 24 or (B, D) 48 h of co-culture between treatment at either 25 or 100 nM and PBMCs. Levels of (A, B) IL-1β and (C, D) tumor necrosis factor are shown. All data is presented as mean ± SEM with n = 3 per treatment group. Significance between treatments at the same concentration is shown and was analyzed using one-way ANOVA with Sidak's multiple comparisons test to analyze differences. *p<0.05; **p<0.01; ***p<0.001; ****p<0.0001; ns=non-significant.

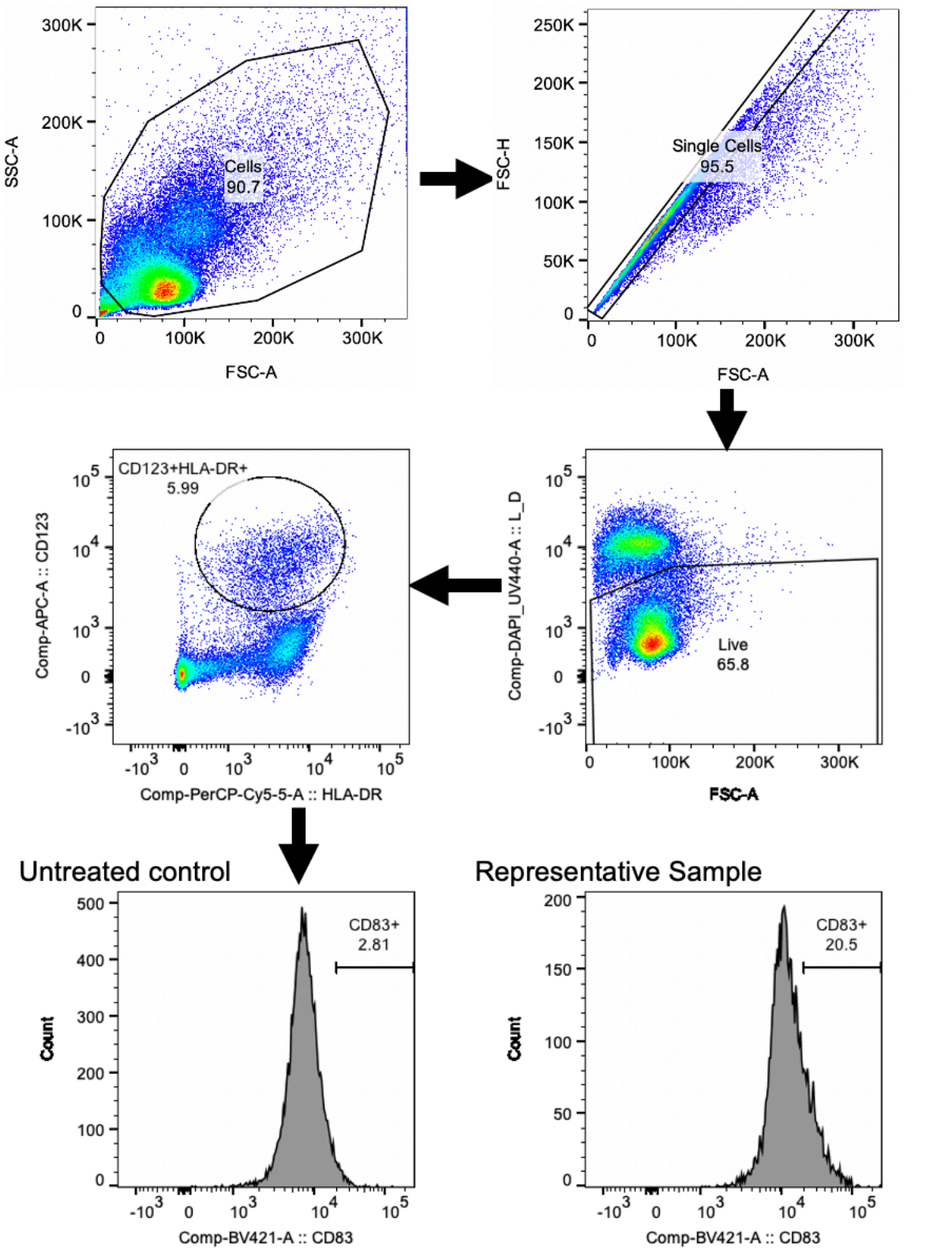

Supplementary Figure S11. Gating Strategy for Figure 3A and 3B demonstrating the presence of co-stimulatory marker CD83.

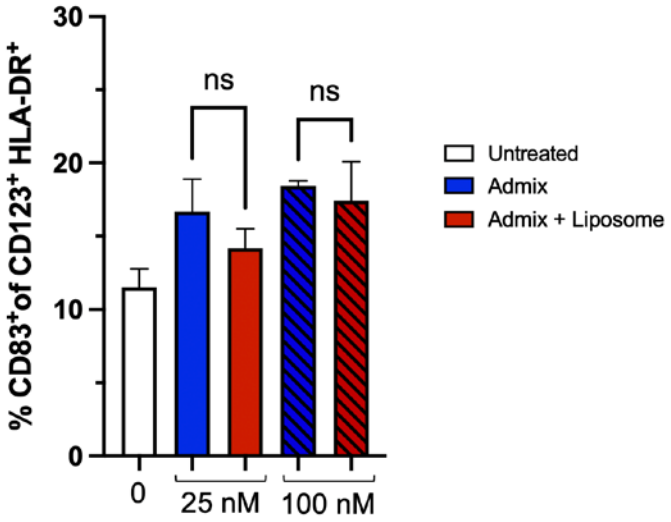

Supplementary Figure S12. Activation of human PBMCs to initiate pDC expression of co-stimulatory marker CD83 with admix or admix supplemented with liposomes (Admix + Liposome). pDCs expressing CD83 is unchanged by the addition of liposomes to the formulation, demonstrating the inert nature and lack of immunostimulatory ability of the liposome itself, thus not contributing any immunostimulation in the SNA vaccine groups. Data is presented as mean ± SEM with n = 3 per treatment group. Significance was analyzed using a one-way ANOVA followed by Sidak's multiple comparisons test. Ns=non-significant.

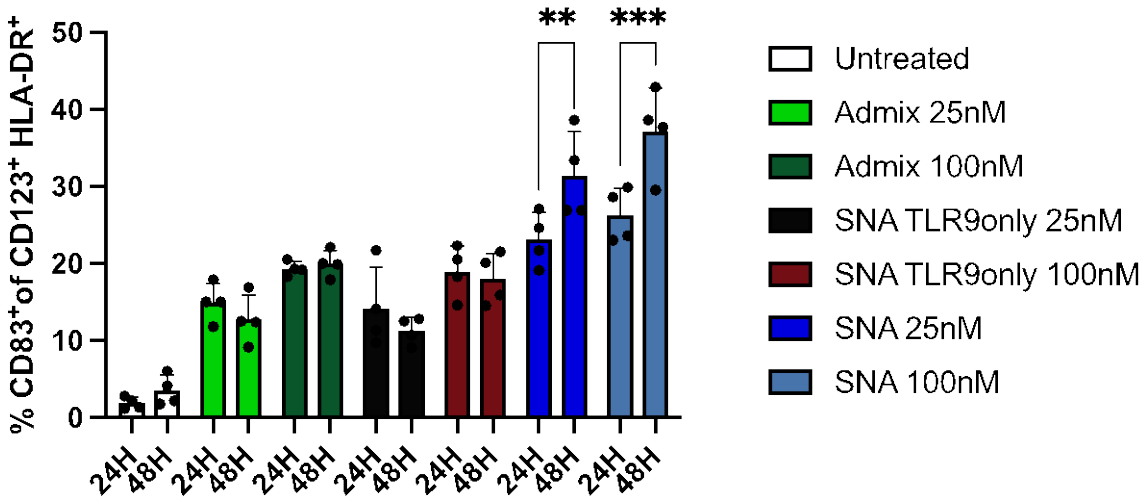

Supplementary Figure S13. Activation of human PBMCs to initiate pDC expression of co-stimulatory marker CD83 after 24 or 48 h. Shown is the proportion of the $CD123^{+}HLA\text{-}DR^{+}$ population that expresses CD83. All data is presented as mean ± SD with n = 4 per treatment group. Significance between time points within each treatment group is shown and was analyzed using two-way ANOVA followed by Sidak's multiple comparisons test. Only comparisons with significance are shown. **p<0.01; ***p<0.001.

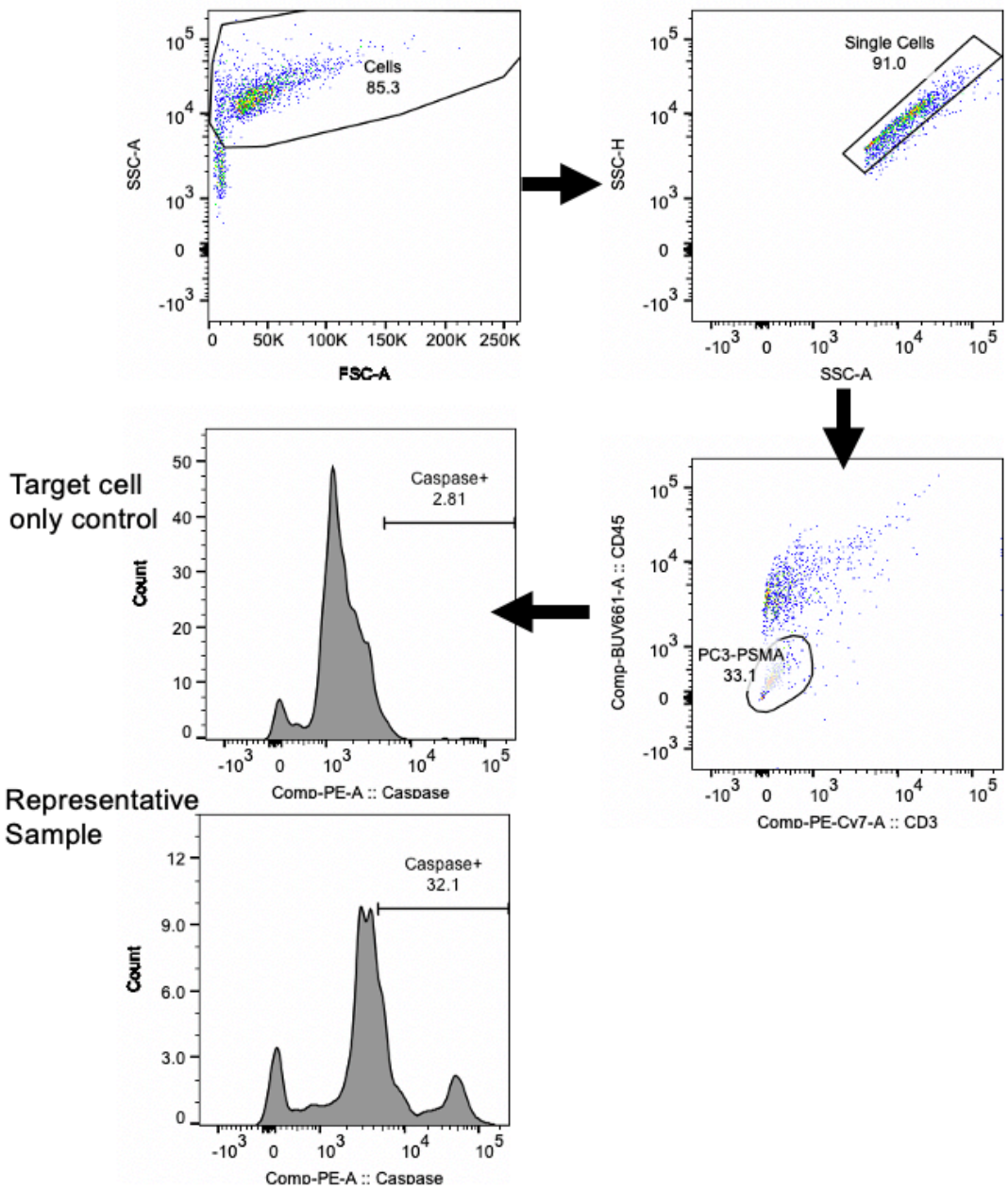

Supplementary Figure S14. Gating Strategy for Figure 3C and 3D demonstrating the percent of the PC3-PSMA target cell population expressing the apoptotic marker Caspase-3.

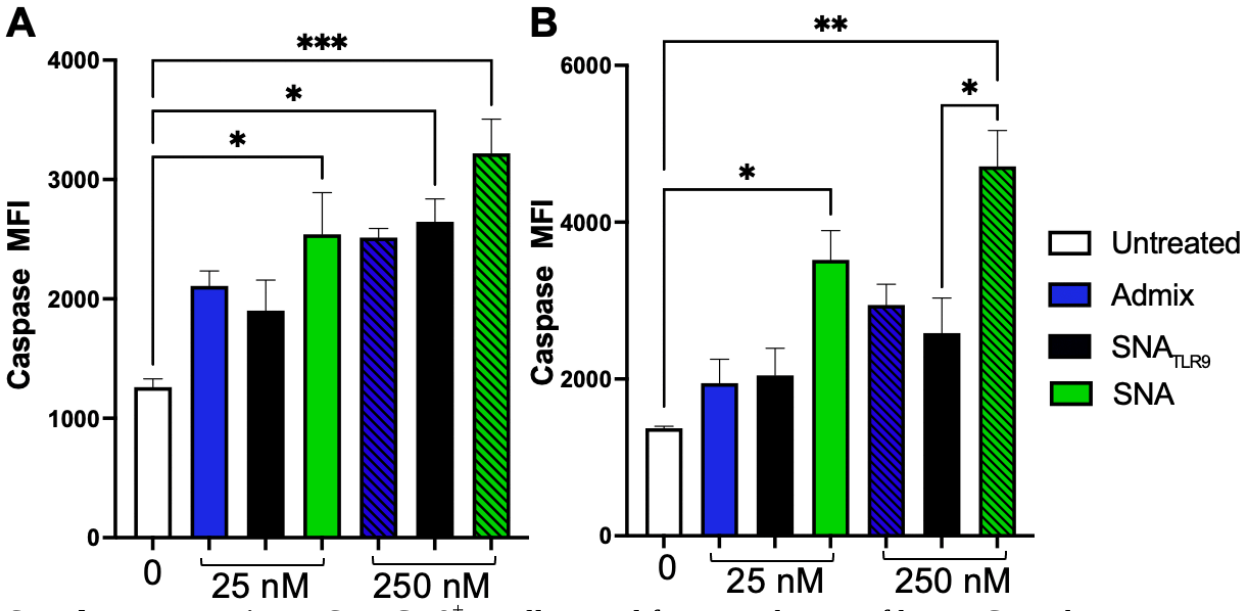

Supplementary Figure S15. $CD8^+$ T cells raised from incubation of hPBMCs with treatment groups for A) 24 or B) 48 h and are targeted against human PCa cells, PC3-PSMA, for 2 h and measured for the expression of the apoptotic marker, Caspase-3. The MFI of Caspase-3 signal amongst the PC3-PSMA population is shown. All data is presented as mean ± SEM with n = 3 - 4 per treatment group. Significance between groups is shown and was analyzed using one-way ANOVA followed by Sidak's multiple comparisons test to analyze differences between treatment groups at each concentration. *p<0.05; **p<0.01; ***p<0.001; ****p<0.0001.